Article

Iridium Luminophore Complexes for Unimolecular Oxygen Sensors

Maria C. DeRosa, Derek J. Hodgson, Gary D. Enright, Brian Dawson, Christopher E. B. Evans, and Robert J. Crutchley

J. Am. Chem. Soc., **2004**, 126 (24), 7619-7626• DOI: 10.1021/ja049872h • Publication Date (Web): 26 May 2004

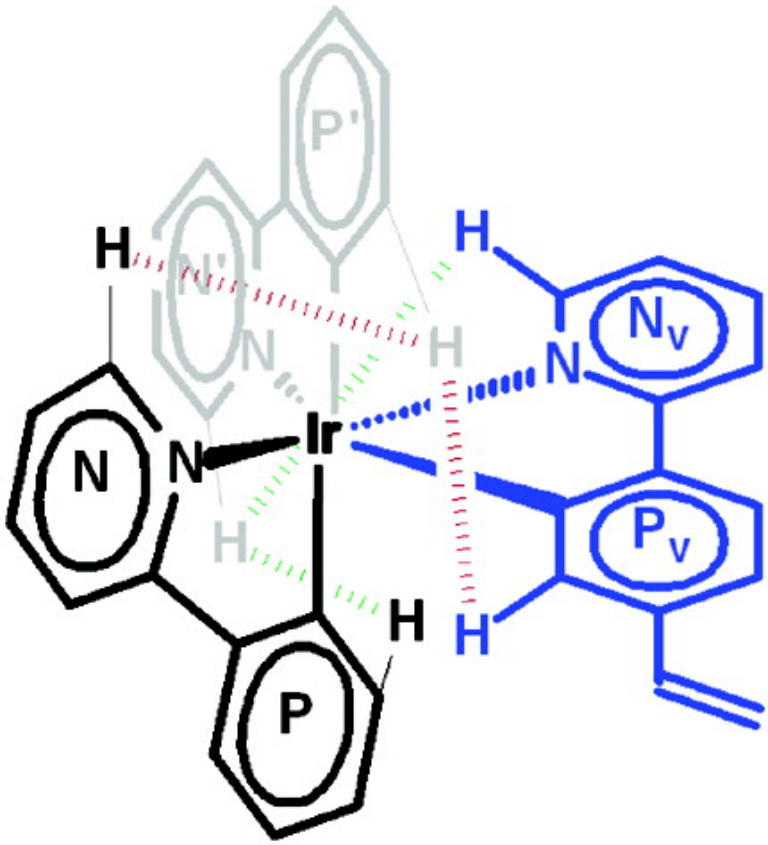

More About This Article

Additional resources and features associated with this article are available within the HTML version:

- Supporting Information
- Links to the 8 articles that cite this article, as of the time of this article download
- Access to high resolution figures

J|A|C|S
ARTICLES
Published on Web 05/26/2004

Iridium Luminophore Complexes for Unimolecular Oxygen Sensors

Maria C. DeRosa,[†] Derek J. Hodgson,[‡] Gary D. Enright,[§] Brian Dawson,*[,‡] Christopher E. B. Evans,*[,§] and Robert J. Crutchley*[,†]

Contribution from the Ottawa-Carleton Chemistry Institute, Carleton University, Ottawa, Ontario, K1S 5B6, Canada, Centre for Biologics Research, Biologics and Genetic Therapies Directorate, Health Canada, Tunney's Pasture, Ottawa, Ontario, Canada K1A 0L2, and National Research Council of Canada, Ottawa, Ontario, Canada K1A 0R6

Received January 8, 2004; E-mail: robert_crutchley@carleton.ca; brian_dawson@hc-sc.gc.ca; chris.evans@coven.net

Abstract: In this study, a series of novel luminescent cyclometalated Ir(III) complexes has been synthesized and evaluated for use in unimolecular oxygen-sensing materials. The complexes $Ir(C6)_2(vacac)$, **1**, $Ir(ppy)_2(vacac)$, **2**, *fac*-$Ir(ppy)_2(vppy)$, **3**, and *mer*-$Ir(ppy)_2(vppy)$, **4**, where C6 = Coumarin 6, vacac = allylacetoacetate, ppy = 2-phenylpyridine, and vppy = 2-(4-vinylphenyl)pyridine, all have pendent vinyl or allyl groups for polymer attachment via the hydrosilation reaction. These luminophore complexes were characterized by NMR, absorption, and emission spectroscopy, luminescence lifetime and quantum yield measurements, elemental analysis, and cyclic voltammetry. Complex **1** was structurally characterized using X-ray crystallography, and a series of 1-D (^1H, ^{13}C) and 2-D ($^1H-^1H$, $^1H-^{13}C$) NMR experiments were used to resolve the solution structure of **4**. Complexes **1** and **3** displayed the longest luminescence lifetimes and largest quantum efficiencies in solution ($\tau = 6.0\ \mu s$, $\phi = 0.22$ for **1**; $\tau = 0.4\ \mu s$, $\phi = 0.2$ for **3**) and, as result, are the most promising candidates for future luminescence-quenching-based oxygen-sensing studies.

Introduction

Luminescence-quenching-based oxygen sensors find applications in a variety of areas from medicine to chemical and environmental analysis.[1] One notable application of these materials is in flow visualization; in this field, these sensors are commonly known as pressure-sensitive paints (PSPs). PSPs are gaining widespread acceptance as the technology of choice for use in surface pressure distribution measurements for aerodynamic applications.[2] These paints are typically composed of an oxygen-sensitive luminescent compound dispersed in an oxygen-permeable polymer matrix. An ideal luminophore complex for oxygen sensing should fulfill several key requirements: efficient emission (high quantum yield) for improved sensitivity, long excited state lifetime (from hundreds of nanoseconds to microseconds) to be quenched efficiently by oxygen, as well as excellent photostability and resistance to singlet oxygen. Ancillary properties such as a large Stokes shift and long wavelength excitation energies, that is, in the visible range, improve the applicability of a luminophore to oxygen sensing. Some of the most promising luminophores for oxygen sensing are based on cyclometalated iridium(III) complexes, and several have recently been investigated for PSP applications.[3]

The dispersed nature of the luminescent molecules in many PSP formulations can lead to problems of aggregation within the paint or leaching from the oxygen-permeable matrix.[4] Recently, work from Manners and Winnik et al. has established that the covalent attachment of a luminophore to the polymer matrix can help lessen these problems and can result in improved behavior over analogous dispersed systems.[5] In an earlier work, we have shown that the hydrosilation reaction is an effective methodology for the creation of unimolecular oxygen sensors from nonionic vinyl-bearing luminophores and hydride-terminated siloxane polymers.[6] This study describes a series of cyclometalated Ir(III) complexes for use in pressure-sensitive paints: $Ir(C6)_2(vacac)$, **1**, $Ir(ppy)_2(vacac)$, **2**, *fac*-$Ir(ppy)_2(vppy)$, **3**, and *mer*-$Ir(ppy)_2(vppy)$, **4**, where C6 = Coumarin 6, vacac = allylacetoacetate, ppy = 2-phenylpyridine, and vppy = 2-(4-vinyl)-phenylpyridine. These compounds represent the two main types of complex luminophores currently employed in PSP, those with ligand-based emission, and those with charge-transfer

[†] Carleton University.
[‡] Health Canada.
[§] National Research Council of Canada.

(1) Amao, Y. *Microchim. Acta* **2003**, *143*, 1 and references therein.
(2) (a) Bell, J. H.; Schairer, E. T.; Hand, L. A.; Mehta, R. D. *Annu. Rev. Fluid Mech.* **2001**, *33*, 155. (b) Hubner, J. P.; Caroll, B. F.; Schanze, K. S.; Ji, H. F.; Holden, M. S. *AIAA J.* **2001**, *39*, 654. (c) Engler, R. H.; Klein, C.; Trinks, O. *Meas. Sci. Technol.* **2000**, *11*, 1077. (d) Taghavi, R.; Raman, G.; Bencic, T. *Exp. Fluids* **1999**, *26*, 481. (e) Dowgwillo, R. M.; Morris, M. J.; Donovan, J. F.; Benne, M. E. *J. Aircr.* **1996**, *33*, 109.
(3) (a) Vander Donckt, E.; Camerman, B.; Hendrick, F.; Herne, R.; Vandeloise, R. *Bull. Soc. Chim. Belg.* **1994**, *103*, 207. (b) Amao, Y.; Ishikawa, Y.; Okura, I. *Anal. Chim. Acta* **2001**, *445*, 177. (c) Gao, R.; Ho, D. G.; Hernandez, B.; Selke, M.; Murphy, D.; Djurovich, P. I.; Thompson, M. E. *J. Am. Chem. Soc.* **2002**, *124*, 14828. (d) Carlson, B.; Khalil, G.; Gouterman, M.; Dalton, L. *Polym. Prepr.* **2002**, *43*, 590.
(4) (a) Lu, X.; Manners, I.; Winnik, M. A. *Macromolecules* **2001**, *34*, 1917. (b) Klimant, I.; Wolfbeis, O. S. *Anal. Chem.* **1995**, *67*, 3160. (c) Hubner, J. P.; Carroll, B. F.; Schanze, K. S.; Ji, H. F. *Exp. Fluids* **2000**, *28*, 21.
(5) Wang, Z.; McWilliams, A. R.; Evans, C. E. B.; Lu, X.; Chung, S.; Winnik, M. A.; Manners, I. *Adv. Funct. Mater.* **2002**, *12*, 415.
(6) DeRosa, M. C.; Mosher, P. J.; Yap, G. P. A.; Focsaneanu, K.-S.; Crutchley, R. J.; Evans, C. E. B. *Inorg. Chem.* **2003**, *42*, 4864.

(i.e., metal-to-ligand or ligand-to-metal)-based emission. In addition, these luminophores are functionalized with pendent vinyl or allyl groups to allow for the covalent attachment of these complexes to hydride-containing silicones via transition-metal-catalyzed hydrosilation.

X-ray crystallography has been established as the principal technique in structure determination, and one seldom finds a study of any novel inorganic or organometallic complex that does not include a crystal structure in its characterization. Unfortunately, the process of growing an X-ray quality crystal is an arduous one, and many systems are not conducive to crystal growth. In these instances, alternate methods of structural characterization must be explored. NMR spectroscopy is undoubtedly one of the most powerful techniques in structure elucidation with its 1-D and 2-D experiments routinely employed to resolve the molecular structure of proteins and DNA complexes.[7] Organometallic and coordination chemists typically apply ^{1}H and ^{13}C NMR spectroscopy to confirm the presence of organic ligands on their complexes, but there are few examples where NMR spectroscopy is used to determine the three-dimensional structure of their systems.[8] In this study, we also present a unique example where a series of 1-D (^{1}H, ^{13}C) and 2-D (^{1}H−^{1}H, ^{1}H−^{13}C) NMR experiments served to resolve the solution structure of *mer*-Ir(ppy)$_2$(vppy), **4**.

Experimental Section

Iridium(III) chloride hydrate was purchased from Strem, and 2-phenylpyridine, silver triflate, allylacetoacetate, and Coumarin 6 were purchased from Aldrich. $[Ir(ppy)_2Cl]_2$ and $[Ir(C_6)_2Cl]_2$ were prepared according to published procedures.[9]

Cyclic voltammetry was performed with a BAS CV-27 voltammograph and a BAS X-Y recorder. A double-jacketed cell was fitted with a Teflon lid incorporating the three electrodes and an argon bubbler and was attached to a Haake D8-G circulating bath to maintain the temperature at 25 °C. Platinum disk working and counter electrodes (BAS, 1.6 mm diameter), a silver wire pseudo-reference with ferrocene as an internal reference, and 0.1 M tetrabutylammonium hexafluorophosphate (TBAH; twice recrystallized in 1:1 EtOH/water) as the supporting electrolyte were all used. NMR spectra were acquired either on a Bruker AMX-400 at ambient temperatures processed using X-32 computer software UXNMR 920801 or on a Bruker Avance 700 at 284 K, operating at 16.35 T (corresponding to 700.13 MHz for ^{1}H and 176.07 ^{13}C), processed using XWIN NMR 3.0. All experiments used CD_2Cl_2 or acetone-d_6 from Cambridge Isotopes Ltd. and Sigma-Aldrich and were referenced to solvent resonances at 5.32 and 2.05 ppm, respectively. Elemental analyses were performed by Canadian Microanalytical Service, Ltd. of Delta, B. C., Canada. Electron impact mass spectrometry (EI-MS) was performed at the University of Ottawa Mass Spectrometry Center. Absorption and steady-state emission spectra were acquired in dry CH_2Cl_2 or dry toluene on a Cary 5 UV−vis−NIR spectrophotometer and a Photon Technology International version 1.23 luminescence spectrometer, respectively, at ambient temperatures. Time-resolved fluorescence decays were obtained by excitation with the third harmonic of a Surelite Nd:YAG laser (355 nm, 6 ns, ≤25 mJ). All experiments were done in static 0.7 × 0.7 cm^2 fused silica cuvettes, following purging with N_2 gas for 15 min. For the quantum yield determinations, the N_2 purged samples were optically matched to an Ir(ppy)$_3$ standard using a Varian Cary 1E spectrophotometer. Toluene was used as the solvent for all lifetime and quantum yield measurements.

[Ir(C6)$_2$(vacac)], 1. $[Ir(C6)_2Cl]_2$ (0.2 g, 0.17 mmol, FW 1154.20 g mol^{-1}) and silver triflate (0.09 g, 0.35 mmol, 256.06 g mol^{-1}) were dissolved in acetone (40 mL) and refluxed under argon for 2 h. The cloudy orange solution was cooled to room temperature and gravity-filtered to remove AgCl. To the filtrate was added allylacetoacetate (vacac) (64 μL, 0.43 mmol) and triethylamine (0.5 mL). The solution was stirred overnight at room temperature under argon. Solvent-stripping to dryness yielded a deep orange solid which was purified using a short silica gel column, eluting with diethyl ether. The first bright orange band was collected and solvent-stripped to dryness. The product was recrystallized by slow diffusion of hexanes into a concentrated dichloromethane solution, yielding red-orange X-ray quality crystals of [Ir(C6)$_2$(vacac)], **1** (120 mg, 0.12 mmol, 34% yield, FW 1032.23 g mol^{-1}). Anal. Calcd as the monosolvate $C_{35}H_{26}N_3Ir\cdot CH_2Cl_2$: C, 51.61; H, 4.06; N, 5.02. Found: C, 51.94; H, 4.02; N, 5.17. ^{1}H NMR (acetone-d_6, 400 MHz): 7.98 (t, 2H, 8 Hz), 7.58 (d, 1H, 8 Hz), 7.46 (d, 1H, 8 Hz), 7.23 (m, 4H), 6.19 (t, 2H, 2 Hz), 6.02 (dd, 2H, 9 Hz, 2 Hz), 5.91 (m, 2H), 5.65 (m, 1H), 4.97 (m, 2H), 4.38 (qtd, 2H, 17 Hz, 5 Hz, 1.5 Hz), 4.28 (s, 1H), 3.21 (dq, 8H, 7 Hz, 2.6 Hz), 1.55 (s, 3H), 0.90 (dt, 12H, 7 Hz, 2.5 Hz). UV−vis: $\epsilon_{445} = 7.79 \times 10^4$ M^{-1} cm^{-1}; $\epsilon_{473} = 8.65 \times 10^4$ M^{-1} cm^{-1}. CV: 0.69 V vs ferrocene (MeCN, 0.1 M TBAH).

X-ray Structural Determination of 1. The single-crystal diffraction data were collected at 173 K on a Bruker SMART CCD diffractometer with Mo Kα radiation (0.71073 Å). The program SMART was used for collecting frames of data, indexing reflections, and determination of lattice parameters; SAINT was used for integration of the intensity of reflections and scaling. SADABS was used for absorption correction, and SHELXTL was used for space group and structure determination, and least-squares refinements on F^2.[10] Hydrogen atoms were placed in calculated positions and constrained to ride with the atoms with which they were bonded. Problems in refinement convergence were largely due to solvent disorder.

[Ir(ppy)$_2$(vacac)], 2. $[Ir(ppy)_2Cl]_2$ (0.5 g, 0.47 mmol, FW 1072.11 g mol^{-1}) and silver triflate (0.13 g, 0.94 mmol, FW 256.06 g mol^{-1}) were dissolved in acetone (40 mL) and refluxed under nitrogen for 2 h. The cloudy yellow solution was cooled and gravity-filtered to remove AgCl. Allylacetoacetate (vacac) (174 μL, 1.18 mmol, FW 142.16 g mol^{-1}) and triethylamine (0.5 mL) were added to the filtrate. The solution was then stirred overnight at room temperature under nitrogen. After solvent-stripping to dryness, the dark yellow solid was purified on a short silica gel column, eluting with dichloromethane. The first bright yellow band was collected and solvent-stripped to dryness. The product was recrystallized by slow diffusion of hexanes into a

(7) For example, see: (a) Radha, P. K.; Patel, P. K.; Hosur, R. V. *Biochemistry* **1998**, *37*, 9952. (b) Gelasco, A.; Lippard, S. J. *Biochemistry* **1998**, *37*, 9230. (c) Kurutz, J. W.; Lee, K. Y. C. *Biochemistry* **2002**, *41*, 9627. (d) Hemmi, H.; Yoshida, T.; Kumazaki, T.; Nemoto, N.; Hasegawa, J.; Nishioka, F.; Kyogoku, Y.; Yokosawa, H.; Kobayashi, Y. *Biochemistry* **2002**, *41*, 10657. (e) Dowd, T. L.; Rosen, J. F.; Li, L.; Gundberg, C. M. *Biochemistry* **2003**, *42*, 7769. (f) Ying, J.; Ahn, J.-M.; Jacobsen, N. E.; Brown, M. F.; Hruby, V. J. *Biochemistry* **2003**, *42*, 2825. (g) Ojha, R. P.; Dhingra, M. M.; Sarma, M. H.; Shibata, M.; Farrar, M.; Turner, C. J.; Sarma, R. H. *Eur. J. Biochem.* **1999**, *265*, 35. (h) Eichmüller, C.; Tollinger, M.; Kräutler; B.; Konrat, R. *J. Biomol. NMR* **2001**, *20*, 195. (i) Chen, J. M.; Nelson, F. C.; Levin, J. I.; Mobilio, D.; Moy, F. J.; Nilakantan, R.; Zask, A.; Powers, R. *J. Am. Chem. Soc.* **2000**, *122*, 9648. (j) Mondelli, R.; Scaglioni, L.; Mazzini, S.; Bolis, G.; Ranghino, G. *Magn. Reson. Chem.* **2000**, *38*, 229.

(8) (a) Bortolin, M.; Bucher, U. E.; Rüegger, H.; Venanzi, L. M.; Albinati, A.; Lianza, F.; Trofimenko, S. *Organometallics* **1992**, *11*, 2514. (b) Kortes, R. A.; Stringfield, T. W.; Ward, M. S.; Lin, F.-T.; Shepherd, R. E. *Inorg. Chim. Acta* **2000**, *304*, 60. (c) Reger, D. L.; Gardinier, J. R.; Smith, M. D.; Pellechia, P. J. *Inorg. Chem.* **2003**, *42*, 482. (d) Proudfoot, E. M.; Mackay, J. P.; Karuso, P. *Dalton Trans.* **2003**, *2*, 165. (e) Macchioni, A. *Eur. J. Inorg. Chem.* **2003**, *2*, 195. (f) Zuccaccia, C.; Bellachioma, G.; Cardaci, G.; Macchioni, A. *J. Am. Chem. Soc.* **2001**, *123*, 11020.

(9) (a) Sprouse, S.; King, K. A.; Spellane, P. J.; Watts, R. J. *J. Am. Chem. Soc.* **1984**, *106*, 6647−6653. (b) Nonoyama, M. *Bull. Chem. Soc. Jpn.* **1974**, *47*, 767−768. (c) Nonoyama, M. *J. Organomet. Chem.* **1974**, *82*, 271−276. (d) Lamansky, S.; Djurovich, P.; Murphy, D.; Abdel-Razzaq, F.; Lee, H.-E.; Adachi, C.; Burrows, P. E.; Forrest, S. R.; Thompson, M. E. *J. Am. Chem. Soc.* **2001**, *123*, 4304−4312.

(10) Blessing, R. *Acta Crystallogr.* **1995**, *A51*, 33−38.

concentrated dichloromethane solution, yielding a golden yellow microcrystalline solid [Ir(ppy)$_2$(vacac)], **1** (330 mg, 0.514 mmol, 55% yield, FW 641.75 g mol^{-1}). Anal. Calcd as the semihydrate $C_{35}H_{26}N_3Ir\cdot 0.5H_2O$: C, 53.53; H, 4.03; N, 4.30. Found: C, 53.41; H, 3.83; N, 4.34. ^{1}H NMR (acetone-d_6, 400 MHz): 8.64 (m, 2H), 8.08 (m, 2H), 7.93 (m, 2H), 7.65 (d, 2H, 8 Hz), 7.35 (m, 2H), 6.76 (t, 2H, 7.6 Hz), 6.60 (m, 2H), 6.23 (d, 2H, 7.6 Hz), 5.67 (m, 1H), 4.98 (m, 2H), 4.73 (s, 1H), 4.25 (qtd, 2H, 12 Hz, 5.6 Hz, 1.5 Hz), 1.72 (s, 3H). UV−vis: $\epsilon_{257} = 4.32 \times 10^4$ M^{-1} cm^{-1}; $\epsilon_{400} = 3.92 \times 10^3$ M^{-1} cm^{-1}. CV: 0.47 V vs ferrocene (MeCN, 0.1 M TBAH).

2-(4-Vinylphenyl)pyridine (vppyH). Potassium-*tert*-butoxide (21.8 mL, 1.0 M solution in THF) was added dropwise through a septum into a flame-dried Schlenk flask containing a cloudy white suspension of methyl triphenylphosphonium bromide (3.9 g, 10.91 mmol, FW 357.24 g mol^{-1}) in diethyl ether (100 mL). The yellow mixture was cooled in an ice/water bath and stirred for 30 min. A solution of 4-(2-pyridyl)benzaldehyde (1 g, 5.46 mmol, FW 183.21 g mol^{-1}) in diethyl ether (15 mL) was then added slowly over 10 min via cannula. The resultant solution was shielded from light, allowed to gradually warm to room temperature, and stirred overnight. Distilled water (50 mL) was added to the solution, and the ether layer was separated and washed three times with aliquots of distilled water (3 × 50 mL). The yellow ether layer was then dried over $MgSO_4$. Solvent-stripping to dryness resulted in a pale yellow oil which was purified by column chromatography on silica gel, eluting with 15% diethyl ether in hexanes (0.47 g, 2.6 mmol, 47% yield, FW 180.23 g mol^{-1}). ^{1}H NMR (CD_2Cl_2, 400 MHz): 8.66 (1H, m), 8.00 (2H, d, 8.3 Hz), 7.77 (2H, m), 7.53 (2H, d, 8.5 Hz), 7.23 (1H, m), 6.78 (1H, dd, 17.6 Hz, 10.9 Hz), 5.85 (1H, dd, 17.6 Hz, 0.8 Hz), 5.30 (1H, m). MS (EI): $M^+ = 181$.

***fac*-[Ir(ppy)$_2$(vppy)], 3.** 2-(4-Vinylphenyl)pyridine (1.0 g, 5.5 mmol, FW 180.23 g mol^{-1}), [Ir(ppy)$_2$Cl]$_2$ (0.8 g, 0.75 mmol, FW 1072.11 g mol^{-1}), and silver triflate (0.38 g, 1.5 mmol, FW 256.06 g mol^{-1}) were all dissolved in 2-ethoxyethanol (15 mL) and heated using an oil bath under nitrogen to 95 °C overnight. The deep yellow solution was cooled and gravity-filtered to remove the gray AgCl precipitate. The filtrate was solvent-stripped to dryness and was purified by column chromatography (silica gel) using 2:1 hexanes/diethyl ether as the eluent to remove unreacted vppy. The mobile phase was switched to 1:1 hexanes/diethyl ether to elute the bright yellow product band, which was solvent-stripped to dryness to yield [Ir(ppy)$_2$(vppy)], **3** (0.09 g, 0.13 mmol, 18% yield, FW 680.83 g mol^{-1}). Anal. Calcd as the monohydrate $C_{35}H_{26}N_3Ir\cdot H_2O$: C, 60.15; H, 4.04; N, 6.01. Found: C, 60.56; H, 4.12; N, 5.64. ^{1}H NMR (CD_2Cl_2, 700 MHz): 7.95 (m, 3H), 7.69 (m, 6H), 7.59 (m, 3H), 7.04 (m, 1H), 6.94 (m, 5H), 6.81 (m, 5H), 6.46 (dd, 1H, 17.49 and 10.84 Hz), 5.49 (d, 1H, 17.60 Hz), 5.03 (d, 1H, 10.87 Hz). UV−vis: $\epsilon_{287} = 4.24 \times 10^4$ M^{-1} cm^{-1}; $\epsilon_{290} = 1.13 \times 10^4$ M^{-1} cm^{-1}. CV: 0.31 V vs ferrocene (CH_2Cl_2, 0.1 M TBAH).

***mer*-[Ir(ppy)$_2$(vppy)], 4.** [Ir(ppy)$_2$Cl]$_2$ (0.5 g, 0.47 mmol, FW 1072.11 g mol^{-1}) and silver triflate (0.13 g, 0.94 mmol, FW 256.06 g mol^{-1}) were dissolved in acetone (40 mL) and refluxed under nitrogen for 2 h. The cloudy yellow solution was cooled and gravity-filtered to remove AgCl. To the filtrate were added vinylpyridine (vppyH) (0.35 g, 1.9 mmol, FW 180.23 g mol^{-1}) and triethylamine (0.5 mL). The solution was then stirred overnight at room temperature under nitrogen. After being solvent-stripped to dryness, the dark yellow solid was purified on a short silica gel column, eluting with dichloromethane. The first bright yellow/orange band was collected and solvent-stripped to dryness. The product was recrystallized by slow diffusion of hexanes into a concentrated dichloromethane solution, yielding a golden yellow microcrystalline solid [Ir(ppy)$_2$(vppy)], **4** (220 mg, 0.33 mmol, 70% yield, FW 680.83 g mol^{-1}). Anal. Calcd as the solvate $C_{35}H_{26}N_3Ir\cdot 0.2(C_6H_{14})$: C, 62.29; H, 4.16; N, 6.02. Found: C, 62.51; H, 4.56; N, 5.48. ^{1}H NMR (CD_2Cl_2, 700 MHz): 8.14 (N6, dd, 1H, 5.86 and 1.59 Hz), 7.98 (N$_v$3, d, 1H, 8.25 Hz), 7.96 (N$_v$6, dd, 1H, 5.54 and 1.60 Hz), 7.87 (N3, N3′, d, 2H, 8.13 Hz), 7.77 (P$_v$3, d, 1H, 5.56 Hz), 7.75 (P3, d, 1H, 7.56 Hz), 7.71 (P3′, dd, 1H, 7.89 and 1.31 Hz), 7.68 (N$_v$4, ddd, 1H, 7.81, 7.78, and 1.72 Hz), 7.65 (N6′, d, 1H 5.89 Hz), 7.61 (N4, ddd, 1H, 7.78, 7.76, and 1.63 Hz), 7.57 (N4′, ddd, 1H, 7.79, 7.76, and 1.49 Hz), 7.12 (P$_v$4, dd, 1H, 8.10 and 1.94 Hz), 7.01 (P4, ddd, 1H, 7.39, 7.53, and 1.38 Hz), 6.96 (P5, ddd, 1H, 7.19, 7.21, and 1.23 Hz), 6.94 (N$_v$5, ddd, 1H, 7.28, 5.82, and 1.38 Hz), 6.93 (P4′, ddd, 1H, 7.43, 7.31, and 1.54 Hz), 6.91 (P$_v$6, d, 1H, 1.90 Hz), 6.86 (P5′, ddd, 1H, 7.38, 7.36, and 1.40 Hz), 6.81 (N5′, ddd, 1H, 7.40, 5.99, and 1.41 Hz), 6.80 (N5, ddd, 1H, 7.36, 5.96, and 1.43 Hz), 6.61 (P6, dd, 1H, 7.20 and 1.36 Hz), 6.51 (P$_{vA}$, dd, 1H, 17.64 and 10.892 Hz), 6.45 (P6′, dd, 1H, 7.64 and 1.21 Hz), 5.52 (P$_{vC}$, dd, 1H, 17.63 and 1.28 Hz), 5.06 (P$_{vB}$, dd, 1H, 10.22 and 1.27 Hz). ^{13}C NMR (CD_2Cl_2, 176 MHz): 177.76 (P$_v$1), 175.18 (P1), 170.60 (N2), 168.10 (N$_v$2), 167.98 (N2′), 159.71 (P1′), 153.59 (N6), 151.61 (N$_v$6), 148.26 (N6′), 146.02 (P$_v$2), 145.26 (P2), 142.73 (P2′), 138.34 (P$_{vA}$), 138.22 (P$_v$5), 137.12 (N$_v$4), 136.35 (P$_v$6), 136.20 (N4), 134.78 (N4′), 132.96 (P6), 130.80 (P6′), 130.23 (P5), 129.92 (P5′), 124.84 (P$_v$3), 124.59 (P3), 124.44 (P3′), 122.83 (N$_v$5 or N5′), 122.69 (N5), 121.91 (N5′ or N$_v$5), 121.35 (P4), 119.70 (N$_v$3), 119.51 (P$_v$4), 119.291 (P4′), 119.18 (N3 or N3′), 118.93 (N3 or N3′), 113.37 (P$_{vBC}$). UV−vis: $\epsilon_{274} = 4.86 \times 10^4$ M^{-1} cm^{-1}; $\epsilon_{390} = 7.99 \times 10^3$ M^{-1} cm^{-1}. CV: 0.25 V vs ferrocene (CH_2Cl_2, 0.1 M TBAH).

Results and Discussion

Synthesis of 1−4. The reaction of the chloride-bridged dimer [Ir(C6)$_2$Cl]$_2$ with the vacac ligand in the presence of silver triflate led to the synthesis of the mononuclear iridium complex **1**. Complex **2** was synthesized in a similar fashion using [Ir(ppy)$_2$Cl]$_2$ as a starting material. In both cases, the dimers were confirmed by NMR spectroscopy to be in the trans configuration.

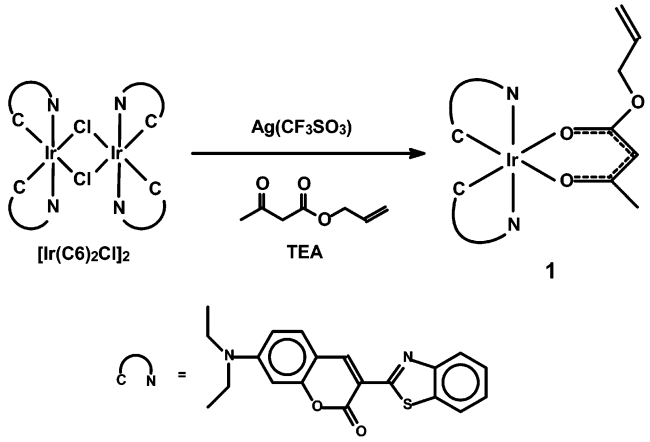

Complex **3** was synthesized from the addition of vppyH to the chloride-bridged dimer [Ir(ppy)Cl]$_2$ in 2-ethoxyethanol at elevated temperatures (95 °C), using silver triflate to scavenge the chloride ions. The low yield of **3** (18%) prompted a modification of the reaction conditions. The solvent was changed to acetone, and triethylamine was added to help deprotonate the vppyH ligand. These new reaction conditions led to the synthesis of the novel complex **4** in good yield (70%). Elemental analysis and ^{1}H NMR spectroscopy confirmed the purity and formula of the two complexes, and thus the possibility that **3** and **4** were analogous to the facial and meridional isomers of Ir(ppy)$_3$ was explored.

Tris-complexes with asymmetric ligands present the possibility of preparing either facial (*fac*) or meridional (*mer*) isomers. A recent study by Thompson et al. has been the only study of

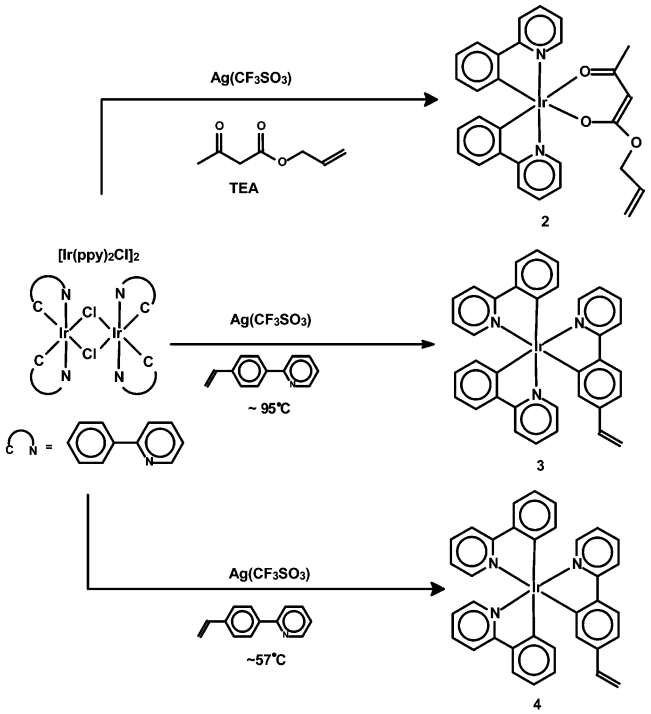

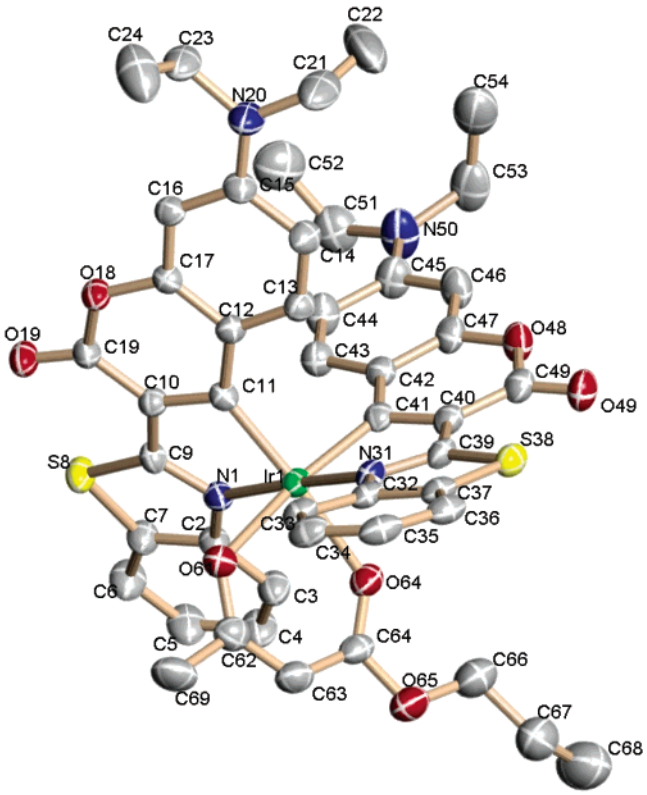

Figure 1. ORTEP diagram of **1**·(CH_2Cl_2) (30% probability). Hydrogen atoms and molecules of solvation have been removed for clarity. Selected bond lengths (Å) and angles (deg): Ir−C41, 1.9912(13); Ir−C11, 1.981-(2); Ir−N1, 2.0488(14); Ir−N31, 2.0386(14); Ir−O61, 2.1246(11); Ir−O64, 2.1404(17); O61−Ir−O64, 87.68(6); N1−Ir−O61, 82.74(5); C41−Ir−O61, 172.37(7); C11−Ir−N1, 80.29(7).

Table 1. X-ray Crystallographic Data for **1**·(CH_2Cl_2)

empirical formula	$C_{48}H_{45}Cl_2IrN_4O_7S_2$
formula weight	1117.10 g mol^{-1}
crystal system	monoclinic
space group	*P*21/*c*
unit cell dimensions	$a = 14.5249(9)$ Å; $\beta = 124.978(10)°$
	$b = 17.4530(11)$ Å
	$c = 22.1208(14)$ Å
volume	4594.8(5) $Å^3$
calculated density	1.615 Mg/m^3
l	0.71073 Å
R1 (F_o^2)	0.0434
wR2 (F_o^2)	0.1034
Z	4
absorption coefficient	3.169 mm^{-1}

mer isomers of d^6 trischelates to date.[11] In this case, high temperatures (refluxing glycerol ~200 °C) were required to synthesize the *fac* isomer, while the *mer* isomer could be prepared using glycerol at 140−145 °C. Because the synthesis of **4** is carried out at low temperature, it can be suggested that this is the kinetically favored product, while the higher reaction temperature used in 2-ethoxyethanol allows for **3**, the thermodynamically favored product, to be formed. A *fac* isomer would have all three phenyl ligands on the same face of the molecule, trans to a pyridyl nitrogen. This is likely the more thermodynamically favored structure due to the strong trans influence of the anionic phenyl ligand. Further confirmation of this is shown in the sections on electronic spectroscopy and cyclic voltammetry.

Structural Analysis of 1 and 4. Single crystals of **1** were grown by diffusion of hexanes into concentrated dichloromethane solutions, and its structure was unambiguously confirmed by X-ray crystallography. The molecular structure of **1**·(CH_2Cl_2) is given as Figure 1, and X-ray crystallographic data have been placed in Table 1.

Attempts to grow X-ray quality crystals of **3** and **4** to confirm the structure of the two isomers have so far yielded only powders. We attempted to apply 1-D and 2-D NMR techniques using a 700 MHz instrument to determine the structures of **3** and **4**, particularly to verify that they were indeed "*mer*" and "*fac*" isomers. The effective C_3 symmetry of the *fac* isomer should lead to a simpler ^{1}H NMR spectrum, while the C_1 symmetry of the *mer* isomer would yield a much more complicated pattern. Unfortunately, the spectral overlap present in the *fac* isomer precluded complete NMR analysis. The ^{1}H and ^{13}C NMR spectra of **3** can be found in Figures 2 and S1, respectively. The ^{1}H NMR spectra of **1** and **2** can also be found in the Supporting Information, Figures S2 and S3, respectively. One key feature of all the ^{1}H NMR spectra is the presence of resonance assigned to the vinyl and allyl groups that are crucial to the hydrosilation attachment reaction.

The suspected "*mer*" isomer **4** was investigated using a series of ^{1}H and ^{13}C NMR experiments. Each of the proton resonances was assigned using a combination of 1-D and 2-D techniques. The 1-D ^{1}H NMR spectrum of the complex (Figure 3) confirmed the correct number of protons (26) and displayed minimal overlap among the peaks, which is essential to the unambiguous assignment of the structure. The signals at 6.51, 5.53, and 5.07 ppm are representative of the vinyl protons Pv_A, Pv_C, and Pv_B, respectively (see Chart 1). These peaks were easily assigned due to their large coupling constants through the double bond ($^3J_{trans}$ = 17 Hz, and $^3J_{cis}$ = 10 Hz). The signal at 6.91 was

(11) Tamayo, A. B.; Alleyne, B. D.; Djurovich, P. I.; Lamansky, S.; Tsyba, I.; Ho, N. N.; Bau, R.; Thompson, M. E. *J. Am. Chem. Soc.* **2003**, *125*, 7377−7387.

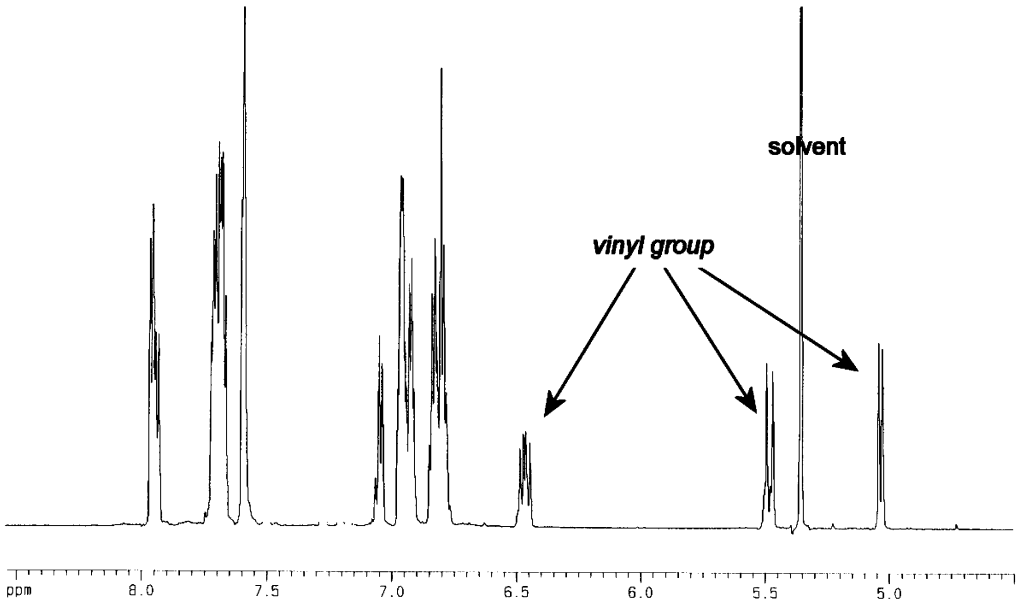

Figure 2. ^{1}H NMR spectrum (700 MHz) of **3** in CD_2Cl_2. The resonances corresponding to the vinyl moiety are highlighted.

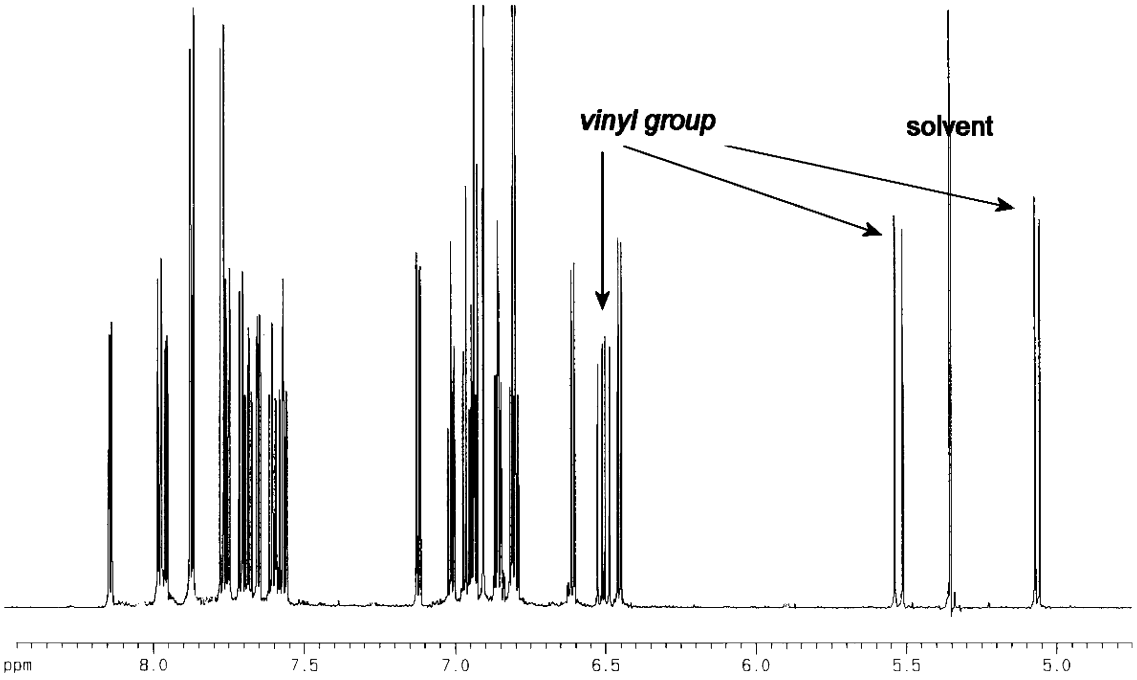

Figure 3. ^{1}H NMR spectrum (700 MHz) of **4** in CD_2Cl_2. The resonances corresponding to the vinyl moiety are highlighted.

assigned to Pv_6 as it is split solely by a meta proton with a ^4J coupling constant of ca. 1.5 Hz. The remaining protons were assigned to their position in the bicyclic system via their splitting patterns and coupling constants. The protons that are in the 4th and 5th positions in a phenyl ring have a splitting pattern of doublet of triplets (dt), or a doublet of doublet of doublets (ddd), whereas those in the 3rd and 6th positions show a doublet of doublet (dd) pattern. The protons at the 3rd and 6th positions of the pyridine portion of the ring system were distinguished using the difference in coupling constants ($^3J = 5-6$ Hz for protons adjacent to the nitrogen, and $^3J = 7-8$ Hz for the other protons). The proton assignments were confirmed using correlated spectroscopy (COSY; Figure S4) and total correlated spectroscopy (TOCSY; Figure S5).

The ^{13}C NMR spectrum of **4** confirmed the presence of 23 unique carbons in the molecule (Figure S6). Through the use of DEPT 135 (distortionless enhancement by polarization transfer; Figure S7), each carbon resonance was identified as either quaternary, CH, or CH_2. Only one CH_2 carbon was found, with a chemical shift of 113.37 ppm, assigned to the vinyl carbon (P_{vBC}). Heteronuclear multiple quantum coherence (HMQC; Figure S8) was used to assign the carbon shifts to the corresponding proton shift, while the assignment of the quaternary carbons and the attachment of the rings in each bicyclic

Chart 1. Diagram of *mer*-[Ir(ppy)$_2$(vppy)], **4**, Indicating the Numbering Scheme Used in Assigning the ^{1}H NMR Spectrum (All Resonances Are Assigned in Table 2)

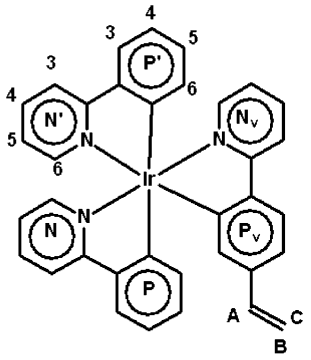

Table 2. ^{1}H and ^{13}C Chemical Shifts for **4** and Assignments

^{1}H chemical shift (ppm)	assignment	^{13}C chemical shift (ppm)	assignment
8.14	N6	177.76	P$_v$1
7.98	N$_v$3	175.18	P1
7.96	N$_v$6	170.60	N2
7.87	N3 and N3′	168.10	N$_v$2
7.77	P$_v$3	167.98	N2′
7.75	P3	159.71	P1′
7.71	P3′	153.59	N6
7.68	N$_v$4	151.61	N$_v$6
7.65	N6′	148.26	N6′
7.61	N4	146.02	P$_v$2
7.57	N4′	145.26	P2
7.12	P$_v$4	142.73	P2′
7.01	P4	138.34	P$_{vA}$
6.96	P5	138.22	P$_v$5
6.94	N$_v$5	137.12	N$_v$4
6.93	P4′	136.35	P$_v$6
6.91	P$_v$6	136.20	N4
6.86	P5′	134.78	N4′
6.81	N5′	132.96	P6
6.80	N5	130.80	P6′
6.61	P6	130.23	P5
6.51	P$_{vA}$	129.92	P5′
6.45	P6′	124.84	P$_v$3
5.52	P$_{vC}$	124.59	P3
5.06	P$_{vB}$	124.44	P3′
		122.83	N5′ or N$_v$5
		122.69	N5
		121.91	N5′ or N$_v$5
		121.35	P4
		119.70	N$_v$3
		119.51	P$_v$4
		119.29	P4′
		119.18	N3 or N3′
		118.93	N3 or N3′
		113.37	P$_{vBC}$

system were determined by heteronuclear multiple bond coherence (HMBC; Figure S9). See Table 2 for a list of ^{1}H and ^{13}C chemical shifts and their assignments.

Once all resonances were assigned, it was then possible to use ROESY experiments (rotating frame Overhauser spectroscopy; see Figure 4) to determine through-space interring interactions and, in turn, the configuration of the ligands about the iridium center. Figure 5 shows the key inter-ring correlations used to assign the final structure. For a correlation to exist, the two interacting protons must be within 5 Å of one another.[12] Using this technique, the following interactions could be established: N6 with P6′ and P$_v$6, P6 with N6′ and N$_v$6. These interactions can only occur in the meridional structural isomer shown in Figure 5 and its mirror image.

Electrochemistry of 1−4. All complexes showed quasi-reversible oxidations in acetonitrile or dichloromethane (see Table 3) that ranged from 0.25 to 0.69 V vs the ferrocene/ferrocenium redox couple, in agreement with literature data.[9d,11,13] Oxidation of Ir(III) cyclometalated compounds tends to be reversible when iridium centered, while oxidation of HOMOs with considerable σ-bond orbital contributions are irreversible;[14] thus, these oxidations are assigned to the iridium(IV/III) couple. The trend in the electrochemistry data corresponds well with the emission data for the complexes with predominantly metal-to-ligand charge-transfer (MLCT)-based emission (see section on solution electronic spectroscopy).

mer-Ir(III) tris-cyclometalates have been shown to be easier to oxidize than their facial analogues by 50−100 mV.[11] The electrochemistry of **3** and **4** (Table 3) concurs with these findings with a 60 mV difference in Ir(IV/III) couples, which could be rationalized by their difference in ligand field strength. In the *mer* isomer, the two anionic phenyl ligands lie trans to one another, which could lead to a lengthening of the Ir−C bonds and a destabilization of the HOMO, allowing for more facile oxidation of the metal center.

Photophysical Properties of 1−4. The photophysical properties of **1** are dominated by the C6 ligand (see Table 4 and Figure 6). The C6 molecule is a fluorescent laser dye that is emissive at room temperature but shows no noticeable phosphorescence. By cyclometalating C6 with Ir to produce complex **1**, the emission energy shifts from 500 nm for the free dye to 568 nm. Intersystem crossing into the triplet levels of the ligand, assisted by the presence of the heavy iridium center, leads to ligand-based phosphorescence and is responsible for the dramatic energy red-shift seen here and in other C6 complexes.[9d] The electronic spectrum of **1** is characterized by two intense ligand-based absorbances in the blue region.

The absorption spectra of **2**−**4** (see Figure 6) were assigned by analogy to similar phenylpyridine-based complexes[9,13,15] and show intense spin-allowed phenyl- and pyridyl-based $\pi-\pi^*$ bands from 260 to 290 nm with metal-to-ligand (MLCT) transitions from 380 to 450 nm. The MLCT transitions consist of the spin-allowed ^{1}MLCT at higher energies and the formally spin-forbidden ^{3}MLCT at lower energies. The extinction coefficients for the two are comparable in all cases, because the ^{3}MLCT can "steal" intensity from the ^{1}MLCT through spin−orbit coupling induced by the heavy iridium center. Comparison of the absorption spectra of the facial and meridional isomers **3** and **4** reveals several differences. The $\pi-\pi^*$ absorbance in **3** is less intense than in **4** and shows a more pronounced shoulder at lower energy, while the MLCT band envelope of **3** is more sharply defined. These differences mirror those seen in the literature for Ir(III) *fac* and *mer* isomers.[11]

The trend in emission energy for complexes **2**−**4** resembles the trend in their Ir(IV/III) redox couples: the more positive the redox potential, the higher the emission energy. This suggests

(12) Frienkiel, T. A. In *NMR of Macromolecules: A Practical Approach*; Roberts, G. C. K., Ed.; Oxford University Press: Oxford, 1993; p 35−70.
(13) Lamansky, S.; Djurovich, P.; Murphy, D.; Abdel-Razzaq, F.; Kwong, R.; Tsyba, I.; Bortz, M.; Mui, B.; Bau, R.; Thompson, M. E. *Inorg. Chem.* **2001**, *40*, 1704−1711.
(14) Neve, F.; Crispini, A.; Campagna, S.; Serroni, S. *Inorg. Chem.* **1999**, *38*, 2250−2258.
(15) Colombo, M. G.; Brunold, T. C.; Riedener, T.; Güdel, H. U.; Förtsch, M.; Bürgi, H.-B. *Inorg. Chem.* **1994**, *33*, 545−550.

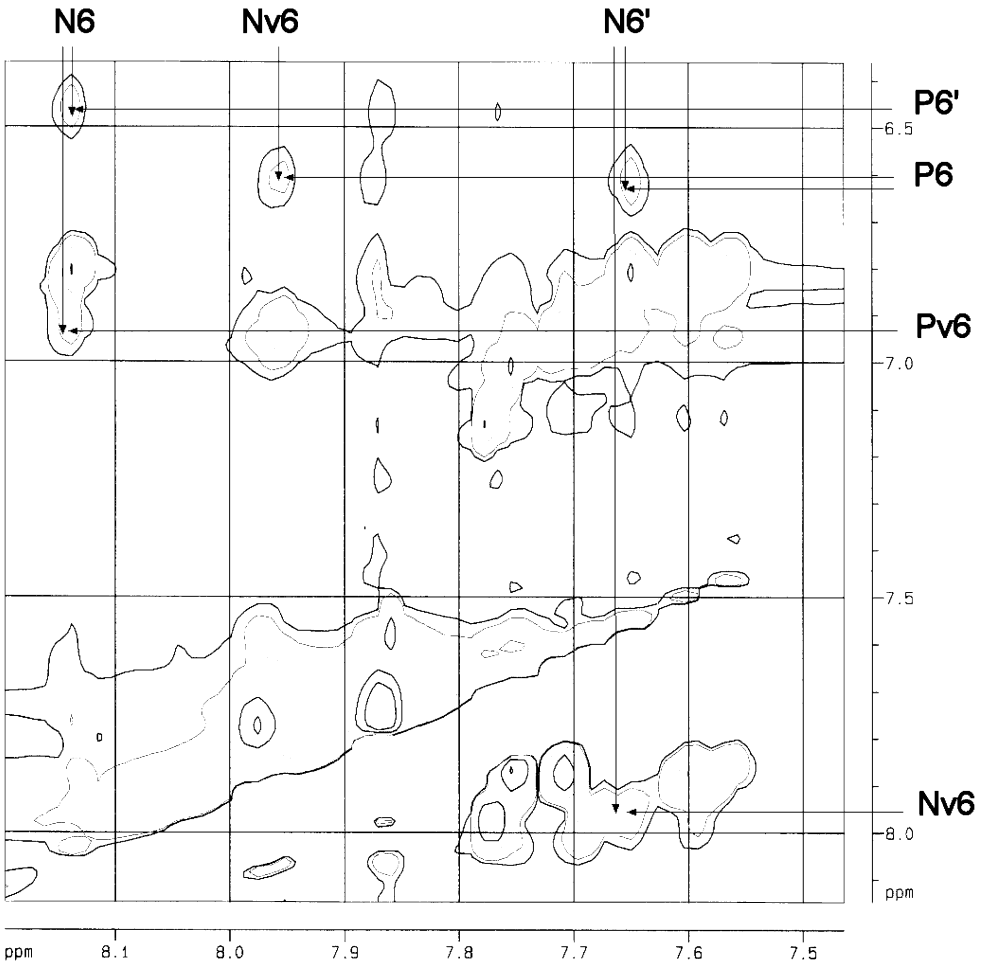

Figure 4. ROESY spectrum (700 MHz) of **4** in CD_2Cl_2 in the region of 6.5−8.2 ppm. The full ROESY spectrum can be found in the Supporting Information (Figure S10).

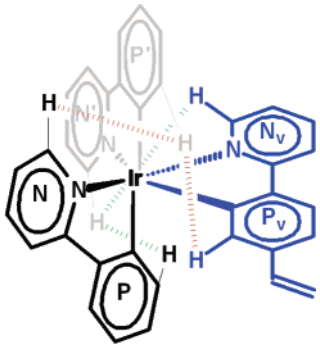

Figure 5. Proposed structure of **4** based on 2-D NMR analysis. Only hydrogens at the 6 positions are shown. Dashed green and red lines indicate key interring correlations determined by ROESY.

the emissive state in these complexes has a large contribution of MLCT character, a reasonable assumption because the emissive states of similar Ir(III) complexes tend to be chiefly MLCT based.[15,16] Complexes **3** and **4** show more structured emission and thus may have some ligand contribution to the emissive state. This is especially seen in the case of **4**, whose emission profile is markedly different from that of $Ir(ppy)_3$.[17] The vinyl group in vinylphenylpyridine leads to greater conjugation in this ligand; thus, its $^3(\pi-\pi^*)$ excited state should be at slightly lower energy than in the phenylpyridine system and may contribute to the emissive state.

Table 3. CV Data for Complexes **1**−**4**

complex	$E_{1/2}$ (V vs Fc/Fc_+)	ΔE_p (mV)
$Ir(C6)_2(vacac)$, **1**[a]	0.69	150
$Ir(ppy)_2(vacac)$, **2**[a]	0.47	60
fac-$Ir(ppy)_2(vppy)$, **3**[b]	0.31	75
mer-$Ir(ppy)_2(vppy)$, **4**[b]	0.25	75

[a] In acetonitrile (0.1 M TBAH). [b] In CH_2Cl_2 (0.1 M TBAH).

Table 4. Electronic Spectroscopy Data for Complexes **1**−**4**

	λ_{max} $\pi-\pi^*$[a] (ϵ)[b]	λ_{max} MLCT (ϵ)	λ_{max} emission	τ (μs) 298 K[e]	ϕ[e]
1	445[d] (7.79×10^4) 474[d] (8.69×10^4)		568,[e] 613[c,e]	6.0	0.22
2	257[d] (4.32×10^4)	400[d] (3.92×10^3) 448[d] (2.76×10^3)	520[f]	0.1	0.02
3	287[f] (4.24×10^4)	384[f] (1.13×10^4) 440[f] (3.90×10^3)	514,[e] 542,[e] 580[c,e]	0.4	0.2
4	274[d] (4.86×10^4)	390[d] (7.99×10^3) 445[d] (3.86×10^3)	535,[d] 572[c,d]	0.2	0.03

[a] Wavelengths in nm. [b] ϵ has units of L mol^{-1} cm^{-1}. [c] Low-energy shoulder. [d] In dichloromethane. [e] In toluene. [f] In acetonitrile.

Table 4 also lists luminescence lifetimes and quantum efficiencies for complexes **1**−**4**. Compound **1** has not only the

(16) Colombo, M. G.; Hauser, A.; Güdel, H. U. *Inorg. Chem.* **1993**, *32*, 3088−3092.
(17) King, K. A.; Spellane, P. J.; Watts, R. J. *J. Am. Chem. Soc.* **1985**, *107*, 1431−1432.

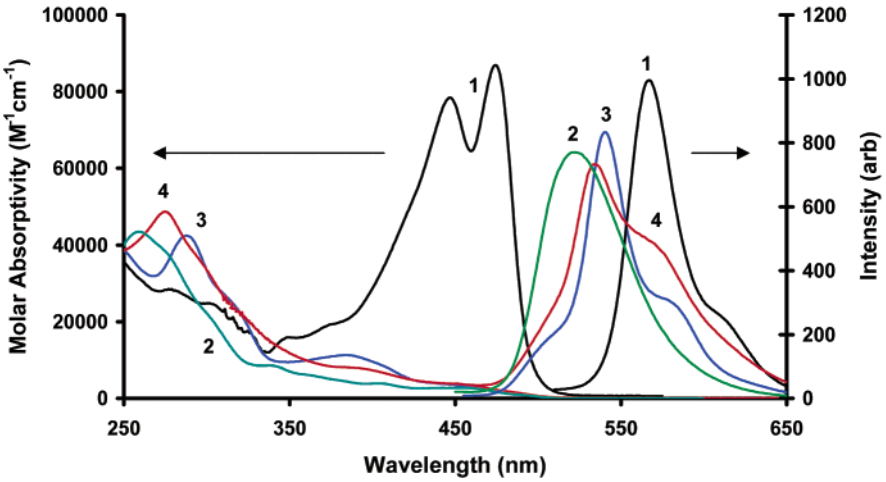

Figure 6. Solution absorption (**1**, **2**, **4**-CH_2Cl_2; **3**-acetonitrile) and emission (**1**, **3**-toluene; **2**-acetonitrile; **4**-CH_2Cl_2) profiles of **1**−**4** (**1**-black, **2**-green, **3**-blue, **4**-red).

longest lifetime and highest quantum efficiency of all complexes, it also enjoys the added advantages of a sizable Stokes shift (3500 cm^{-1}) and intense absorption in the visible which should allow for efficient excitation at longer wavelengths, making it a very promising candidate for future PSP studies.

As expected, the meridional isomer **4** has a shorter luminescence lifetime and a lower quantum yield as compared to its facial analogue **3**. The poorer photophysical properties of **4** could be partially attributed to higher nonradiative rate constants caused by dissociation of the Ir−C bond in the excited state.[11] While **3** possesses a high quantum efficiency and long lifetime as compared to the other phenylpyridine-based complexes in this study, its photophysical properties are less ideal as compared to those of $Ir(ppy)_3$ ($\tau = 2\ \mu s$, $\phi = 0.4$),[17] which has recently been investigated as a luminescent oxygen sensor.[3a,b] Excited-state reactions of the vinyl group could be responsible for an increase in nonradiative decay. The covalent attachment of this luminophore to a hydride-containing silicone polymer via the hydrosilation reaction will result in the saturation of this vinyl group and may lead to improved photophysical properties.

Conclusions

A series of luminescent cyclometalated Ir(III) complexes with suitable pendent ligands for polymer attachment has been synthesized and characterized structurally (X-ray crystallography and NMR spectroscopy), electrochemically (cyclic voltammetry), and spectroscopically (absorption and emission). On the basis of the photophysical properties of the luminophores in solution, sensors based on complexes **1** and **3** are the most promising candidates for PSP studies. Future studies will describe the covalent attachment of these luminophores to hydride-containing silicones and illustrate the advantages of these unimolecular systems over analogous dispersed systems for use in pressure-sensitive paints.

Acknowledgment. We thank Dr. Youssef Mébarki for his assistance with the oxygen sensitivity experiments and Prof. J. C. Scaiano for the use of his equipment for the luminescence lifetime measurements. Financial support by the Natural Science and Engineering Research Council of Canada (NSERC) in the form of a Discovery Grant (R.J.C.) and a postgraduate scholarship (MCD) is gratefully acknowledged. C.E.B.E. thanks the NRC for supporting his research through the Research Associate Program.

Supporting Information Available: 1-D and 2-D NMR spectra of complexes **1**−**4**. Additional figures and X-ray crystallographic files in CIF format for compound **1**. This material is available free of charge via the Internet at http://pubs.acs.org.

JA049872H